JOURNAL OF AGRICULTURAL AND FOOD CHEMISTRY

J. Agric. Food Chem. **2007,** *55,* 6761–6771 **6761**

Viscoelastic Properties of Waxy and Nonwaxy Rice Flours, Their Fat and Protein-free Starch, and the Microstructure of Their Cooked Kernels

ANA M. IBÁÑEZ,*,† DELILAH F. WOOD,§ WALLACE H. YOKOYAMA,§ I. M. PARK,† MARIO A. TINOCO,† CAROL A. HUDSON,§ KENT S. MCKENZIE,# AND CHARLES F. SHOEMAKER†

Food Science and Technology, University of California, Davis, California 95616; Western Regional Research Center, Agricultural Research Service, U.S. Department of Agriculture, Albany, California 94710; and Rice Experiment Station, California Cooperative Rice Research Foundation, Biggs, California 95917

Physicochemistry and structural studies of two types of japonica rice, low amylose Calmochi-101 (CM101) and intermediate amylose M-202 (M202), were conducted to determine similarities and differences between the rices perhaps attributable to amylose content differences. The rheological behavior of the gelation and pasting processes of flours and starches was determined with high accuracy and precision using a controlled stress rheometer. Fat and protein, although minor constituents of milled rice, were shown to have significant effects on the physicochemical and pasting properties of starches and flours. Removal of protein and lipids with aqueous alkaline or detergent solutions caused lower pasting temperatures and higher overall viscosity in both starches, compared with their respective flours. There was less viscosity difference between M202 flour and its starch when isolated by enzymatic hydrolysis of protein. The protease did not reduce internally bound lipids, suggesting that fats help to determine pasting properties of rice flours and their respective starches. Structural integrity differences in individual granules of waxy and nonwaxy rice flours, starches, and whole raw, soaked, and cooked milled grain were revealed by fracture analysis and scanning electron microscopy. Calmochi 101 and M202 did not differ in weight-averaged molar mass (M_w) and root-mean-square radii (R_z) between flours and starches, as determined by high-performance size exclusion chromatography (HPSEC) and multiple-angle laser light scattering (MALLS) (Park, I.; Ibanez, A. M.; Shoemaker, C. F. *Starch* **2007**, *59*, 69−77).

KEYWORDS: Starch structure; amylose content; rheology; pasting properties; electron microscopy; weight-average molar mass

INTRODUCTION

Rice, unlike most cereals, is consumed as the milled whole grain. The relationship between the physicochemical properties of its principal component, starch, and the texture of the cooked kernel has been difficult to determine. The wide range of cooking and textural qualities in rice is largely determined by the relative proportions of amylose and amylopectin in the starch (*1*, *2*). Viscoamylographic analysis is widely used to characterize cereal flours and starches, but cannot predict textural properties of whole cooked rice kernels (*3*, *4*). Differences in formation of starch (amylose) networks under dilute, stirred viscoamylographic conditions and more concentrated, uncooked, whole grains is the most common reason cited. Microscopy indicates that, in addition to rheological properties, differences in starch composition affect mechanical properties. Granule strength may be important in determining viscoamylographic properties when starch and flour are subjected to shearing forces. Microscopy can also show the disposition of protein bodies and matrix proteins that affect cooked rice texture.

Although the physicochemical characteristics of a gelatinized starch gel or paste are largely determined by starch concentration and the structure of the swollen starch granule, lipid and protein also change the rheological properties of cooked starch by interacting with amylose and perhaps amylopectin (*5*). Internal lipid and protein in the granule also affect whole kernel rice texture. Viscosity changes in starch suspensions result from a combination of granule swelling and solubilization and probably occur to some extent in the whole kernel. On cooling, amylose molecules begin to reassociate, forming a precipitate or gel and

* Corresponding author [e-mail amibanez@ucdavis.edu; telephone (530) 752-5325; fax (530) 752-4759].
† University of California.
§ U.S. Department of Agriculture.
# California Cooperative Rice Research Foundation.

10.1021/jf070416x CCC: $37.00
Published on Web 07/18/2007

becoming opaque in the process, called retrogradation or setback. Leached amylose and swollen granules arrange themselves in a special three-dimensional conformation by entanglement of molecule chains, formation of junction zones, and embedding of swollen granules (*6*). Because they form complexes with both amylose and amylopectin, lipids alter the three-dimensional conformation and thus the thermal and mechanical properties of the composite gel (*1*). Whistler and BeMiller (*7*) found that lipid and protein concentrations affect starch pasting properties, either facilitating or hindering junction zone formation, thus affecting the firmness of the gel during pasting. Perez et al. (*8*) identified lipids as a major factor affecting gel consistency and viscosity.

The effect of lipids and proteins on starch pasting properties is studied with different starch isolation methods (*6*). During starch purification, partial hydrolysis of starch components, protein and lipid elimination by alkaline and detergent treatments, and substitution of internal starch lipids associated with dodecylbenzene sulfonate (DoBS, anionic detergent) protein extraction have dramatic effects on starch pasting properties (*9*). However, removal of protein with Pronase or alkaline protease, which effectively reduced protein from 6.47% to below 0.1% without damage to starch granules or reduction of starch lipids, had less effect on pasting properties (*1*, *10*, *11*).

This work compares the physicochemical and pasting properties of waxy and nonwaxy rice flours and starches to evaluate how the isolation method affects the pasting properties of nonwaxy rice starch and to evaluate the microstructures of the isolated starches. Cooked high-amylose rice exhibits less granule disintegration and is harder and less sticky than cooked waxy rice (*12*, *13*). Starch composition also affects the relative rigidity or fragility of uncooked and cooked starch granules. The rheological properties of 'CM101' (waxy) and 'M202' (nonwaxy, low amylose) rice flour and starch during gelatinization, pasting, and retrogradation were measured by a micromethod using a commercial controlled stress rheometer (CSR). The benefits of the rheometer include precise control of shear rate and sample temperature, small sample size (100 mg), measurement of viscosity in fundamental units, and the possibility of continuous measurements throughout a simulated cooking process. Scanning electron microscopy (SEM) was used to observe and understand microscopic changes during cooking of milled waxy and nonwaxy rice kernels. Microscopy studies of granule structure and fracture have shown the relative fragility of waxy grains.

MATERIALS AND METHODS

Milled Calmochi-101 (CM101 japonica, waxy grain) and M202 (japonica, nonwaxy grain) rice were selected from the 1997 crop of the Rice Research Experiment Station, Biggs, CA. Flours were prepared with a laboratory cyclone mill (UDY Corp., Fort Collins, CO) fitted with a 0.5 mm screen.

CM101 and M202 starches were prepared by soaking milled grain in 2 volumes of aqueous 0.3% NaOH for 3 days. The soaked grain was ground in a Waring blender at medium speed for 1 min. The slurry was passed successively through 100, 200, and 400 mesh sieves and extracted repeatedly with aqueous 0.3% NaOH until the extract became negative to protein by the Biuret test; then the starch was washed repeatedly with distilled water until the pH of the supernatant was neutral. The isolated starch was freeze-dried and ground in a mortar to pass through a 100 mesh sieve (*14*).

M202 starch was also prepared by exhaustive extraction of protein with 1.2% sodium dodecyl benzene sulfonate (DoBS). Milled rice was soaked overnight in 3−4 volumes of 1.2% DoBS containing 0.12% Na_2SO_3, homogenized in a Waring blender at medium speed for 5 min, and passed successively through 100, 200, and 400 mesh sieves. The sieved starch was then shaken with 5 volumes of fresh detergent (DoBS−Na_2SO_3) three or four times to extract protein and lipids, and the supernatant was removed by centrifugation until the extract was negative for protein by the Biuret test. The purified starch was washed repeatedly with distilled water until the washing was neutral, freeze-dried (*14*, *15*), and ground in a mortar to pass through a 100 mesh sieve.

M202 starch was also purified by enzymatic protein hydrolysis using Pronase (alkaline protease from *Streptomyces griseus*). Milled rice was soaked in 3 volumes of deionized water for 3 h, ground in a Waring blender at medium speed for 3 min, and passed successively through 100, 200, and 400 mesh sieves to remove all coarse material. The sieved flour was slurried twice with 5 volumes of 0.2% Pronase (45000 UI^{-1}; Calbiochem, San Diego, CA) in 0.03 M phosphate buffer, pH 7.4, for 24 h at 37 °C using 0.02% sodium azide as preservative, and washed five times with deionized water. External lipids were eliminated by soaking the starch slurry twice for 20 min in 5 volumes of water-saturated 1-butanol (WSB). After each extraction, the WSB−starch mixture was centrifuged at 4000 rpm for 10 min (*1*, *10*). The defatted starch was washed six times with distilled water, freeze-dried, and ground in a mortar to pass through a 100 mesh sieve.

Chemical Analyses. Rice flour and starch were analyzed in triplicate. Protein (N × 5.95) was determined by combustion (AACC method 46-30; *16*) using a nitrogen analyzer (Leco, model FP-428, St. Louis, MO). True amylose content was determined by the concanavalin A method (K-AMYL, Megazyme International Ireland Ltd., Ireland) following a simplified procedure (*17*). Total fat was measured using an accelerated solvent extractor (Dionex, model ASE200, Salt Lake City, UT) at 125 °C and 1000 psi, with petroleum ether as the extraction solvent.

Physical Analyses. The average weight of three sets of 100 sound kernels was multiplied by 10 to get the 1000 kernel weight (TKW). Starch granule diameter was determined by particle size analysis (PSA) using a Malvern MasterSizer laser diffraction size analyzer with a 0.1−80 μm range (Malvern Instruments Ltd., Malvern, U.K.). The calculated median diameter, D[v, 0.5] (i.e., the size at which 50% of particles are smaller by volume and 50% larger), was chosen to characterize granule size (*18*). Aqueous rice flour and starch suspensions for PSA were prepared in the same manner as those used for analysis of pasting properties.

Starch molecular weight distributions were determined by size exclusion chromatography with multiple-angle laser light scattering detection as described earlier (*19*). Briefly, 100 mg of starch or flour was dissolved in 50 mM LiBr in DMSO at 95 °C with stirring for 15 min. Samples were centrifuged for 10 min at 10000*g* using a microcentrifuge, and the supernatant was passed through a 0.45 μm filter before analysis. Each sample was prepared in duplicate, and two subsamples were taken from each preparation. Average molar weights were calculated using ASTRA chromatography software (version 1.4, Wyatt Technology, Santa Barbara, CA) for Macintosh using a second-order polynomial fit (*20*).

Pasting Viscosity Profiles. Pasting viscoamylographic profiles for 8% CM101 and M202 rice flour and starch slurries were measured using a controlled stress rheometer (CSR, AR-1000N, TA Instruments, Dover, DE) at a constant shear rate of 200 s^{-1}. The rheometer was fitted with a polysulfone cone (4 cm diameter, 4° angle). The temperature program was as follows: (1) from 45 to 95 °C in 3:45 min; (2) hold at 95 °C for 2:30 min; (3) from 95 to 50 °C in 3:45 min; and (4) hold at 50 °C for 2:30 min. Triplicate aqueous rice flour suspensions (8% w/w) were prepared using 100 mg of rice flour or isolated starch equivalent and 1.25 mL of deionized water. Suspensions were degassed with stirring under vacuum for 15 min. The CSR was operated using rheology navigation software (version 1.1, TA Instruments). Pasting properties measured were initial gelatinization (or onset) temperature (temperature of the initial viscosity increase, °C), peak viscosity (maximum viscosity recorded during heating and holding cycles, Pa·s), hot paste (or trough) viscosity (minimum viscosity after peak, Pa·s), cold (or final) viscosity (viscosity of paste at the end of the test, Pa·s), breakdown (the difference between peak and trough viscosity, indicating breakdown in paste viscosity during the 95 °C holding period, Pa·s), and setback from trough (the difference between

Table 1. Particle Size and Composition of CM101 and M202 Rice Flours and Starches Isolated by NaOH, DoBS, or Pronase Treatment[a]

rice sample	granular size[b] D [v, 0.5], μm	protein[c] (%)	true amylose[d] (%)	total fat[e] (%)
Calmochi101 flour	47.6 ± 0.1	5.8 ± 0.0	1.1 ± 0.1	1.0 ± 0.0
CM101 starch (NaOH)	5.5 ± 0.0	0.0 ± 0.0	1.5 ± 0.2	0.2 ± 0.0
M202 flour	43.7 ± 0.6	5.8 ± 0.0	13.8 ± 0.1	0.4 ± 0.0
M202 starch (NaOH)	6.5 ± 0.2	0.0 ± 0.0	15.9 ± 0.1	0.2 ± 0.0
M202 starch (DoBS)	6.1 ± 0.1	0.0 ± 0.0	15.0 ± 0.6	0.2 ± 0.0
M202 starch (Pronase)	6.0 ± 0.0	0.0 ± 0.0	15.5 ± 0.4	0.3 ± 0.0

[a] Mean ± standard deviation; $n = 3$. [b] Determined by Malvern MasterSizer. D [v, 0.5] = median diameter. [c] N × 5.95, determined by combustion method [AACC (*16*), method 46-30]. [d] Determined by concanavalin A method [Gibson et al. (*17*)]. [e] Determined by accelerated solvent extraction (ASE200, Dionex).

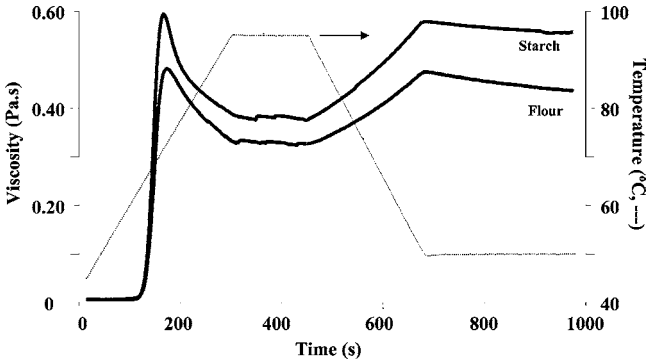

Figure 1. Viscoamylographic profiles of CM101 rice flour and NaOH-isolated starch slurries, measured with a controlled stress rheometer.

final and trough viscosity, indicating starch retrogradation during cooling, Pa•s).

Microscopy. *Preparation of Cooked Rice.* Approximately 5 g of milled rice kernels was cooked in 50 mL of water in a 100 mL beaker (excess water) in the laboratory. Kernels were removed after 5, 10, 15, and 20 min of cooking and prepared for light microscopy or scanning electron microscopy (SEM).

Light Microscopy. Milled kernels were treated in a fixative of 4% glutaraldehyde, 3% formaldehyde, 0.025 M sodium cacodylate, and 1 mM $CaCl_2$ at pH 6.9 in either 50% ethanol (CM101) or distilled water (M202). Different fixation methods were employed due to rapid absorption of water by CM101, which resulted in extensive swelling in aqueous-based fixatives because of the presence of waxy starch. Solvent-based fixatives or the addition of solutes will prevent swelling because such fixatives reduce the available water. Nonwaxy starch inhibits rapid water absorption; thus, M202 did not take up water and swell. Because water is a very small molecule, it can penetrate quickly into samples, whereas fixatives contain much larger molecules and penetrate more slowly. Thus, the overall purpose of balancing the available water of the solution allows the additional time required for penetration of the fixative, which results in stabilization of the samples. Samples were dehydrated with overnight exchanges of methoxyethanol, ethanol, propanol, and butanol, using each solvent undiluted, and then infiltrated with Technovit 7100 plus catalyst at 21 °C (glycol methacrylate resin, Heraeus Kulzer GmbH, Germany). Fixed samples were flat-embedded in Technovit 7100 containing catalyst and hardener. Embedded blocks were cut out of their molds, glued to epoxy holders with cyanoacrylate glue, and sectioned (2−4 μm thick) with glass knives on a Sorvall Porter Blum MT 2 ultramicrotome.

Protein was located by staining slides for 2 min in 0.01% Acid Fuchsin in 1.0% acetic acid. Sections were rinsed in running tap water, air-dried, and mounted in immersion oil (*21*). Proteins appeared red when viewed under fluorescent illumination at 546 nm excitation (exciter filter, BP 546; beam splitter, FT 580; barrier filter, LP 590) and yellowish when viewed at 450−490 nm excitation (exciter filter, 450−490; beam splitter, FT 510; barrier filter, LP 520). Starch granules

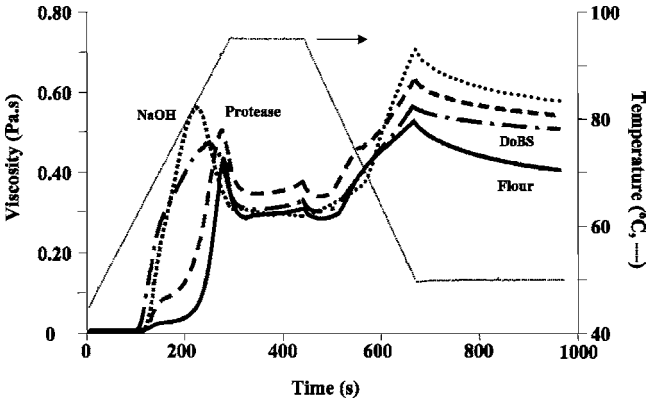

Figure 2. Viscoamylographic profiles for slurries of M202 rice flour (—) and M202 rice starches isolated using NaOH (•••), DoBS (– •–), or protease (- - -), measured with a controlled stress rheometer.

Table 2. Weight-Average Molar Mass (M_W) and Root-Mean-Square Radii (R_z) for Rice Flours and NaOH-Isolated Starches[a]

rice cultivar	M_W (g/mol × 10^8)	R_z (nm)
CM101 flour	1.92 ± 0.09	357 ± 13
CM101 starch (NaOH)	1.75 ± 0.05	359 ± 20
M202 flour	1.23 ± 0.30	346 ± 20
M202 starch (NaOH)	1.05 ± 0.47	249 ± 11
M202 starch (DoBS)	1.30 ± 0.24	333 ± 19
M202 starch (Pronase)	1.27 ± 0.09	357 ± 13

[a] HPSEC-MALLS-DRI system. Samples were analyzed using sets of four columns. Mean ± standard deviation; $n = 3$.

and amylose were detected with I_2KI (*22*), rinsed briefly in running tap water, and mounted in water. Ungelatinized starch granules were located by mounting unstained sections in immersion oil and viewing through crossed polarizers. Finally, cell walls and gelatinized starch were identified by staining in 1% aqueous Congo Red and viewing with a filter set with a 390−420 nm excitation wavelength (exciter filter, 390−420; beam splitter, FT 425; barrier filter, LP 450) (*21*, *22*).

Scanning Electron Microscopy. Dry, raw milled rice grains were fractured with a razor blade and mounted onto aluminum stubs using a mixture of carbon graphite and epoxy. A few kernels of raw rice were soaked in excess water overnight at 4 °C. Soaked kernels were sliced crosswise into ~1 mm thick pieces and placed in a fixative containing 50% ethanol, 4% glutaraldehyde, and 3% formaldehyde buffered with 0.025 M sodium cacodylate and 1 mM $CaCl_2$, pH 6.9. Following fixation, samples were dehydrated in a graded ethanol series (30, 50, 70, 95%, and three exchanges of 100%; 20 min per exchange), fractured in liquid nitrogen (*24*), and critical-point dried in a Tousimis Autosamdri 815 critical-point dryer (Tousimis, Rockville, MD).

Nuclepore track-etch membrane filters (13 mm diameter, 0.2 μm pore size, Whatman, Clifton, NJ) were used to prepare starch samples for SEM. Prior to use, filters were dipped in 0.1% poly(L-lysine) (Sigma Diagnostics, St. Louis, MO), which served as a very thin adhesive layer for the starch granules. Each treated filter was loaded into a 13 mm plastic filter holder (Gelman Sciences, Ann Arbor, MI). Approximately 3 mg of isolated starch was mixed with 5 mL of distilled water and mixed briefly using a Vortex mixer until the particles were well-suspended. One milliliter of the starch−water solution was filtered through a membrane filter, and the filters were allowed to air-dry.

All samples (rice grains or filters) were mounted onto aluminum specimen stubs using two-sided adhesive carbon tabs (Pelco, Redding, CA) and coated with gold−palladium in a Denton Desk II (Denton, NJ) sputter coating unit. Samples were observed in a Hitachi S-4700 field emission scanning electron microscope (SEM) (Hitachi, Tokyo, Japan) using 1−3 kV accelerating voltages. Digital images were captured at 2560 × 1920 pixel resolution.

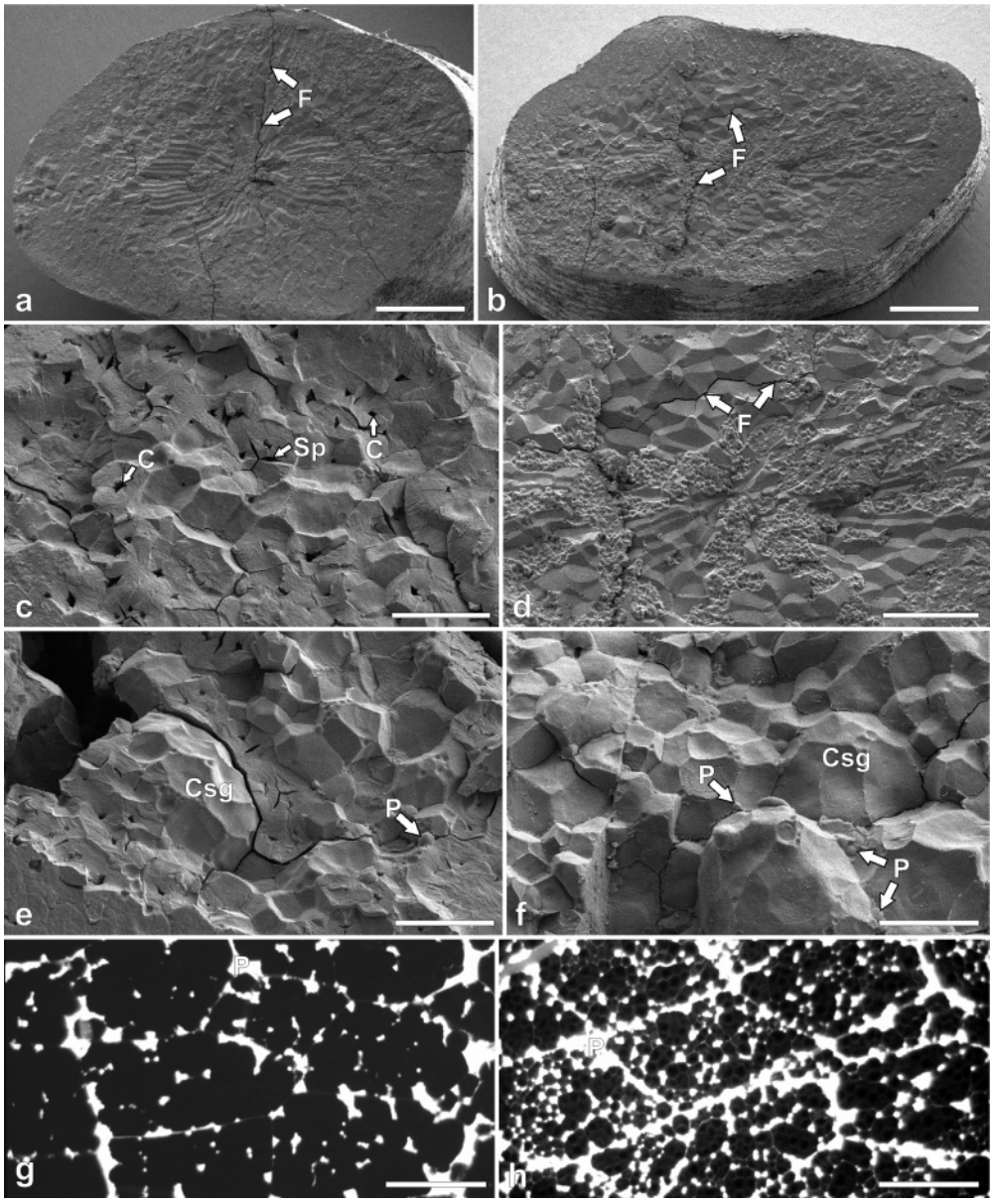

Figure 3. Micrographs of dry, mature, milled grains of CM101 (**a**, **c**, **e**, **g**) and M202 (**b**, **d**, **f**, **h**). Scanning electron micrographs of cross sections approximately midway through the grains show entire cross sections (CM101, **a**; M202, **b**) and central starchy endosperm tissues (CM101, **c**, **e**; M202, **d**, **f**). Fissuring in the grain tends to occur from the outside to the center of the grains (**a**, **b**) along cell walls (**d**). In CM101, central cavities (C) within and spaces (Sp) between individual starch granules are evident in the dry, fractured grain (**c**, **e**), whereas M202 does not exhibit such cavities or spaces in starch granules (**d**, **f**). Sections of milled rice kernels (CM101, **g**; M202, **h**), stained for protein with Acid Fuchsin and viewed under fluorescence illumination at 450–490 nm excitation (exciter filter, 450–490; beam spitter, FT 510; barrier filter, LP 520) show protein distribution (brightest areas). The sections for light microscopy (**g**, **h**) were taken approximately midway between the outer and center portions of the kernels and are closer to the periphery than the scanning electron micrographs shown in panels **e** and **f**. Protein concentration is greater toward the periphery than in the center of the grain; thus, the protein concentration is greater in the areas shown in the light micrographs than in the scanning electron micrographs. C, cavity; CSg, compound starch granule; F, fissure; P, protein body; Sp, space. Scale bars: **a**, **b**, 500 μm; **c**, **e**, **f**, 10 μm; **d**, 250 μm; **g**, **h**, 50 μm.

RESULTS AND DISCUSSION

Size, Shape, and Composition of Grain, Flour, and Starch. We compared particle size, true amylose, and protein and fat compositions of flour and starch prepared by alkali extraction, detergent extraction, or protease treatment from California rice varieties CM101 and M202 (**Table 1**). The *D*[v, 0.5] values of individual starch granules of CM101 were about 15% smaller and hence contained only 60% of the volume of M202 granules. CM101 requires about twice the granules of M202 to have the same weight, which generates about 50% more surface area. The *D*[v, 0.5] of CM101 flour particles was slightly larger than that for M202 particles. The higher number of particles and surface area per unit weight contributed to increased viscosity in CM101 NaOH-extracted starches and to the generally greater viscosities of starches than their respective flours (**Figures 1** and **2**). The various starch preparation methods used for M202 did not alter median granule size, true amylose, or total fat.

Both flours contained 5.8% protein. Although no protein was detected by combustion in isolated starches or in reference starches from commercial corn, rice, and amioca, the reference starches contain 0.26, 0.30, and 0.19% protein, respectively (*25*). We could not detect this because we used too small a sample size for such low nitrogen. Protein bodies were visible in the SEM of NaOH- and DoBS-treated but not Pronase-treated

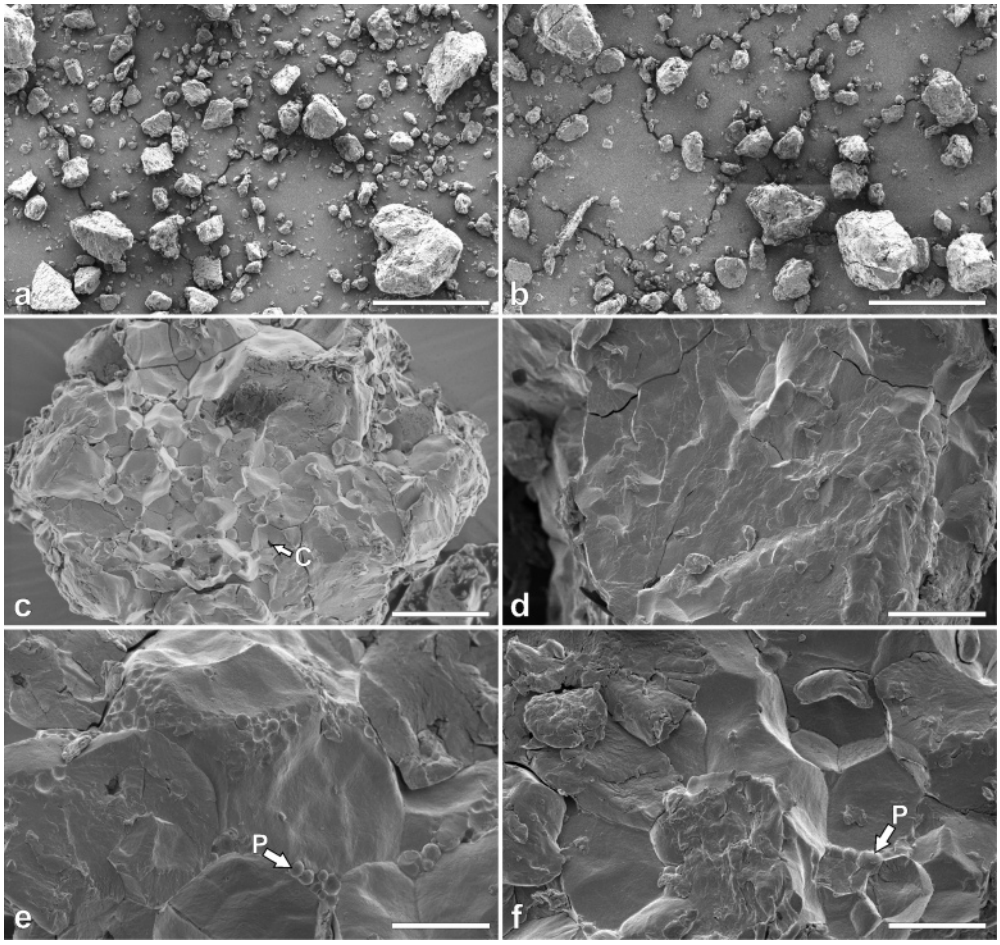

Figure 4. Flours from milled grain of CM101 (**a**, **c**, **e**) and M202 (**b**, **d**, **f**). The flour particles vary drastically in size in both cultivars. Some CM101 starch granules in panel **c** have fractured, whereas others maintain their integrities (**d**). None of the M202 starch granules (**d**, **f**) appear to have fractured. Fracturing indicates that CM101 granules are more fragile than those of M202. C, cavity; P, protein bodies. Scale bars: **a**, **b**, 200 μm; **c**, **d**, 10 μm; **e**, **f**, 5 μm.

starch. True amylose content of CM101 flour was 1.1 ± 0.1%, which is comparable to the 0.85% reported in Calmochi-202 (*26*). True amylose content of M202 was 13.8 ± 0.1%. True amylose contents were greater in the respective starches than in flour, due to removal of protein and fat. Total fat contents of CM101 and M202 flours were 1.0 ± 0.0 and 0.4 ± 0.0%, respectively. Alkaline and detergent starch isolation reduced this to 0.2 ± 0.0% fat. Pronase-isolated M202 rice starch had 0.3 ± 0.0% fat, suggesting that most fat was associated with the surrounding protein matrix. The average molecular weight of CM101 starch was (1.92 ± 0.09) × 10^8 g/mol, which was higher than the (1.23 ± 0.30) × 10^8 g/mol of M202 because it had less amylose (**Table 2**). The TKW values for CM101 and M202 were 19.7 and 22.4 g, respectively, which were similar to reported values for California waxy rices (*26*, *27*).

In addition to physicochemical differences during cooking as revealed by viscoamylography, dry kernels of waxy and nonwaxy rice have visible microstructural differences. Dry fractured CM101 (**Figure 3a**,**c**,**e**) and M202 (**Figure 3b**,**d**,**f**) grains were compared by SEM. Fissures occur in both CM101 (F in **Figure 3a**) and M202 (F in **Figure 3b**). We previously reported such fissures in nonwaxy rices (*28*). The fracture plane in CM101 passed through individual starch granules (**Figure 3c**), unlike in M202 (**Figure 3d**), indicating that interactions between starch molecules within the CM101 granule are weak. CM101 starch granules contained central cavities (C in **Figure 3c**,**e**) as seen previously in waxy rice (*2*) and spaces between starch granules (**Figure 3c**). Central cavities within and spaces between starch granules may contribute to the weak structure of CM101 starch granules. M202 dry-fractured grains (**Figure 3b**,**d**,**f**) tended to break around the compound granules, on the plane of least resistance. The small starch granules were pressed tightly together within compound granules (**Figure 3f**). Protein bodies were also evident in fractured kernels (**Figure 3e**,**f**). The bodies (**Figure 3e**,**f**) apparent in the scanning electron micrographs were identified as proteinaceous by staining sections with Acid Fuchsin and observing the result using fluorescence microscopy (**Figure 3g**,**h**) and then relating the two types of micrographs. To compare the two types of microscopy, one needs to first understand that the results may appear to differ due to the intrinsic differences between the microscopes. Only surfaces, albeit with a very large depth of field, are discernible by scanning electron microscopy. Thus, only the material on the fractured surface will be visible; for example, protein bodies that appear below the surface are not visible. In contrast, the entire thickness of a section is visible using light microscopy. Thus, protein bodies that occur at various depths will appear as if they are in the same plane; therefore, it may appear that more protein bodies are located in the same area when, actually, they are not. One needs also to consider that protein body distribution in rice, as in other grains, varies throughout the grain. Protein bodies are located mostly in the periphery or subaleurone layer of a grain and taper off toward the interior of the grain. The micrographs illustrated here are from different regions of the

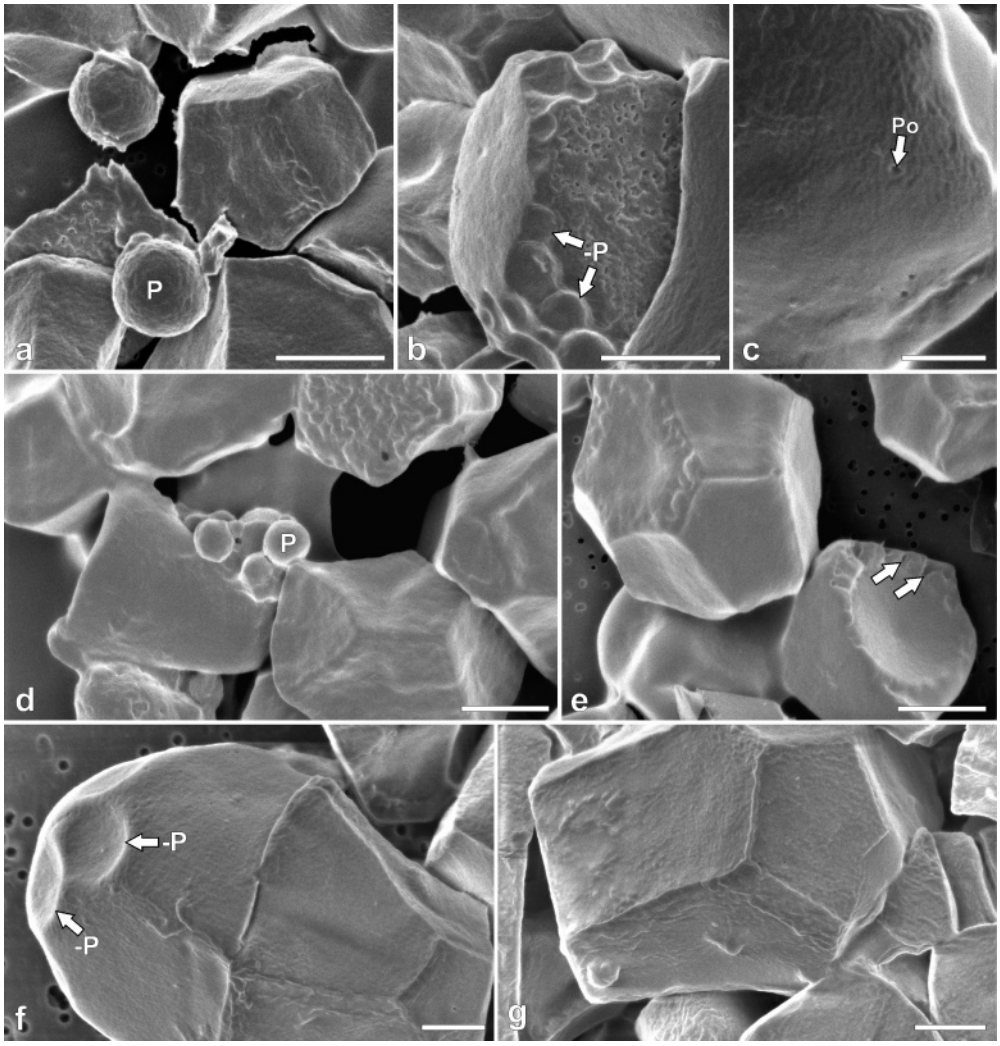

Figure 5. Scanning electron micrographs of isolated starch granules. NaOH-isolated starches are from CM101 (**a**) and M202 (**b**, **c**). Protein bodies are evident in the isolates (**a**). Micropores either become evident following or are formed during isolation (**c**). Starch granules were also isolated from M202 using DoBS (**d**, **e**) or Pronase (**f**, **g**). DoBS did not remove protein (**d**) and produced microchannels (arrows, **e**) in the starch granules. Pronase treatment of M202 (**f**, **g**) removed protein and left starch granules without evident surface modification. P, protein; –P, void after removal of protein: Po, pore. Scale bars: **a**, **b**, 2 μm; **c**, 1 μm; **d**, **e**, 2 μm; **f**, **g**, 1 μm.

grain. The light micrographs (**Figure 3g**,**h**) are taken from a more peripheral location than those in the scanning electron micrographs (**Figure 3e**,**f**). Fracture characteristics could conceivably be affected by protein distribution within the grain. Even though protein concentration is the same in CM101 and M202 (**Table 1**), its distribution differs between the two grains (**Figure 3g**,**h**). Fracture characteristics of waxy and nonwaxy starches suggest that amylose may impart strength to starch granule structure. Surface to volume ratios affect the rheology of suspended particles. We estimated granule median diameter by using a spherical approximation, but granules are not perfect spheres, nor are their surfaces uniform. The flour contained particles of various sizes in both CM101 (**Figure 4a**) and M202 (**Figure 4b**). Individual flour particles of CM101 were rougher and more angular than those of M202. The slight angularity of CM101 may be due to the presence of broken or damaged starch granules. Central cavities within and spaces between starch granules were apparent in flour particles (**Figure 4c**), indicating that milling, like dry-fracturing, caused particles to break through starch granules. Individual flour particles of M202 had more rounded sections, probably due to fracturing around compound starch granules (**Figure 4d**,**f**). These amyloplast packing differences in waxy and nonwaxy rice resemble the chalky and translucent regions, respectively, of nonwaxy rices (*29*). Protein bodies were evident in flour particles of both CM101 (**Figure 4e**) and M202 (**Figure 4f**).

Starch granules isolated using NaOH retained some protein, evident by SEM of CM101 (**Figure 5a**) and verified by specific staining and light microscopy (not shown). Calmochi starch granules were relatively smooth following isolation (**Figure 5a**). NaOH-isolated M202 starch granules were mostly smooth, but occasional starch granules had indentations where numerous protein bodies were located when the grain was intact (**Figure 5b**). Isolated material from M202 also contained protein bodies (not shown), noted by specific staining. Micropores were evident in isolated starch granules of M202 (**Figure 5c**). It is unclear whether micropores were already present on the starch granule surface and NaOH stripped away the exterior of the granule, making the pores visible, or whether the NaOH caused the micropores. Microchannels are reported in corn starch granules, and rice starch granules may have the same structure (*30*). M202 starch granules isolated using DoBS had rough and smooth surfaces (**Figure 5d**,**e**). The surfaces from DoBS starch isolates were smoother than NaOH-isolated preparations, probably due to more effective lipid removal. DoBS isolates contained protein bodies (**Figure 5d**), and channels were evident along angular

Table 3. Pasting Properties for CM101 and M202 Flours and Starches Isolated by NaOH, DoBS, or Protease, Measured by Controlled Stress Rheometer[a]

rice cultivar	initial temperature[b]	peak[c]	hot paste[d]	cool paste[e]	breakdown[f]	setback[g]
CM101 flour	63.4a	0.482a	0.323a	0.467a	0.159a	0.144a
CM101 starch (NaOH)	63.3a	0.594b	0.387b	0.579b	0.217b	0.202b
M202 flour	66.5c	0.430a	0.290a	0.532a	0.140a	0.242a
M202 starch (NaOH)	64.2b	0.580c	0.301ab	0.715d	0.275c	0.414b
M202 starch (DoBS)	62.1a	0.477b	0.304b	0.570b	0.173b	0.265a
M202 starch (protease)	64.9b	0.496b	0.349c	0.614c	0.146a	0.265a

[a] Mean of three determinations. Values within a column not followed by the same letter are significantly different ($P < 0.05$). [b] Initial (or onset) temperature, temperature of the initial viscosity increase, °C. [c] Peak viscosity, maximum viscosity recorded during heating and holding cycles, Pascal·seconds (Pa·s). [d] Hot paste (or trough) viscosity, minimum viscosity after peak, Pa·s. [e] Cool paste (or final) viscosity, viscosity of paste at the end of the test, Pa·s. [f] Breakdown, difference (–) between peak viscosity and trough viscosity; indication of breakdown in viscosity of paste during 95 °C holding period, Pa·s. [g] Setback from trough, difference (–) between final viscosity minus trough viscosity, indication of retrogradation of cooked rice during cooling, Pa·s.

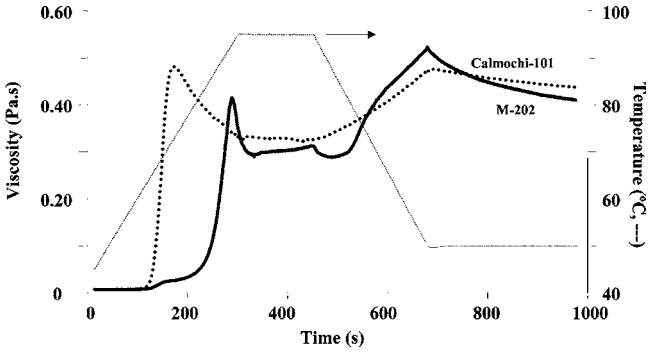

Figure 6. Viscoamylographic profiles for CM101 (•••) and M202 (—) rice flour slurries measured with a controlled stress rheometer.

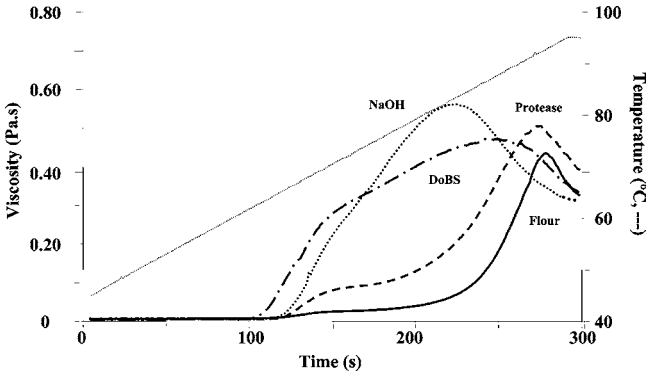

Figure 7. Magnification of the gelatinization onset of the viscoamylographs of **Figure 2**: M202 rice flour (—) and M202 rice starches isolated by NaOH (•••), DoBS (– · –), or protease (- - -) treatments.

portions of some starch granules (arrows, **Figure 5e**). The channels, in contrast to micropores, appear to result from damage during isolation. M202 Pronase-isolated starch was without apparent damage (**Figure 5f**,**g**). The starch granules were very smooth, with some unidentified material adhering (**Figure 5a**), indicating that the enzyme treatment was mild and either that it left residue on the starch surfaces or that residue is a natural part of starch granules. Isolated starch granules had indentations where proteins were located (**Figure 5f**) and angular, smooth areas (**Figure 5g**). Pronase-isolated starch from M202 was protein-free, verified by specific staining. The light and electron microscopy examinations show that starch isolation methods produce physical characteristics such as fissures that are not predicted from composition.

Pasting Properties. The most prominent differences between the viscoamylographic profiles of CM101 and M202 flours are the lower pasting temperature and final and setback viscosities of CM101, due to its very low amylose concentration. Amylose molecules interact to form a matrix that increases viscosity. The waxy CM101 rice flour had higher peak, hot paste, and breakdown viscosities than nonwaxy M202 rice flour (**Table 3**; **Figure 6**). The temperature of the Peltier-controlled sample is shown in **Figures 1** and **2**. These findings agree with reported differences in pasting between waxy and nonwaxy cereal flours (*31*).

Although CM101 starch purified with NaOH had higher overall viscosity than its flour (**Table 3**; **Figure 1**), flour and starch had similar initial gelatinization temperatures. Lim et al. (*11*) noted that protein removal imparts increased viscosity and decreased initial gelatinization temperature to starch. The increased peak viscosity, which represents the maximum starch granule swelling, indicates improved water uptake by starch granules after protein removal. Whereas amylose−lipid interactions have stronger effects on pasting properties, granular lipids may also associate with amylopectin during gelatinization and lower the tendency to retrograde (*1*, *10*). The higher setback viscosity of isolated starch than of Calmochi-101 flour suggests that removal of internal lipids by NaOH facilitated retrogradation in this low-amylose starch. CM101 rice starch had lower initial gelatinization temperature and lower setback than M202 starch isolated in the same way, but similar peak viscosity (**Table 3**). The viscosity data show that M202 starch granules may be damaged by lipid removal during alkaline treatment. The lower initial gelatinization temperature of M202 isolated starch, and its peak viscosity similar to that of CM101 starch is explained by disruption of the amylose−lipid complex in M202 starch. As with flours, low gel formation for CM101 starch due to its very low amylose is reflected in the cool paste viscosity and setback differences between CM101 and M202 starches.

M202 starches purified by alkali, detergent, or enzymes had no detectable protein and demonstrated expected effects of protein removal: lower initial gelatinization temperatures and greater overall viscosities than M202 flour (**Table 3**; **Figure 2**). However, the greater or lesser changes in various pasting properties may reflect different degrees of damage or lipid removal by different treatments. The lower initial gelatinization temperature of M202 starches can be attributed to the absence or disruption of the amylose−lipid complex. Close examination of gelatinization onset of M202 flour and starches (**Figure 7**) shows a delayed viscosity increase in flour, which we attribute to resistance to swelling by the amylose−lipid complexes. In NaOH- and DoBS-treated starches, there is less delay and the viscosity profile is shifted toward that of waxy rice starch (CM101, as in **Figure 1**), likely due to damage of the starch

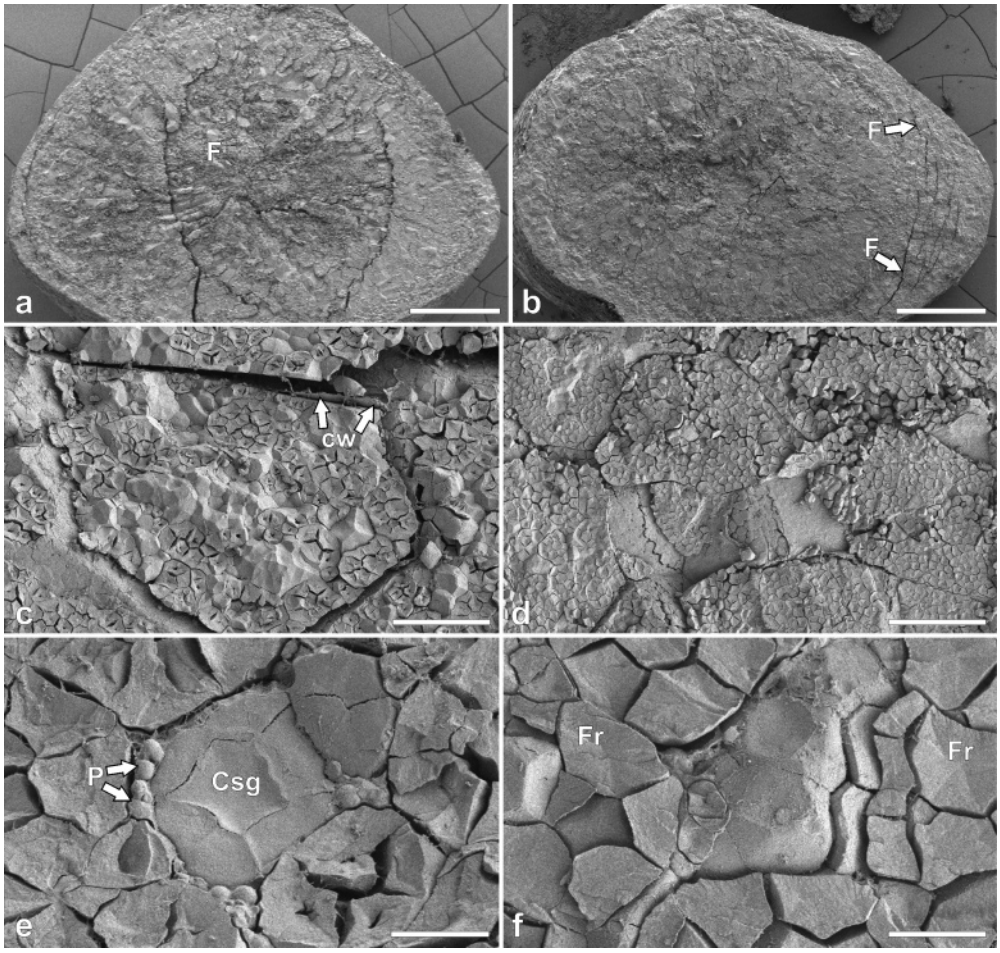

Figure 8. Scanning electron micrographs of soaked, whole, milled grains of CM101 (**a**, **c**, **e**) and M202 (**b**, **d**, **f**). Milled grains fractured approximately midway, showing large fissures in CM101 (**a**) and smaller fissures in M202 (**b**). The central starchy endosperm shows expansion between starch granules, compared to unsoaked endosperm, in both CM101 (**c**, **e**) and M202 (**d**, **f**). Central cavities in the starch granules are evident in CM101 (**c**, **e**) but not in the fractured starch granules of M202 (**d**, **f**). Grains were soaked prior to fixation to force the fracture plane to go through the starch granules rather than between granules as occurred in the dry grain. C, cavity; CSg, compound starch granule; CW, cell wall; F, fissure; Fr, fractured starch granule; P, protein body; Sp, space. Scale bars: **a**, **b**, 500 μm; **c**, 25 μm; **d**, 50 μm; **e**, **f**, 5 μm.

granule's amorphous amylose region. The profile of protease-treated starch shifted very little.

Compared to M202 flour, starch pasting temperature was most affected by DoBS isolation, and least by protease isolation, but changes in most viscosity parameters were greatest for NaOH-isolated M202 starch. This suggests that alkali and detergent may alter the composition or organization of starch granules, thus affecting the pasting properties of isolated starch. Maniñgat and Juliano (*10*) found that DoBS partially replaces internal lipids that bind with the helix structure of starch during the purification. Biliaderis and Juliano (*1*) found that granular internal lipids were eliminated by NaOH treatment of rice starch to remove protein. Protease-purified M202 starch also had a lower initial gelatinization temperature and higher overall viscosity than M202 flour (**Table 3**). However, the generally smaller differences between M202 flour and Pronase-isolated starch suggest that Pronase effectively removed protein without greatly reducing lipids or disrupting starch−lipid complexes.

Light and Scanning Electron Microscopy of Cooked Waxy and Nonwaxy Kernels. Once a sample is wet or soaked, fractures no longer occur preferentially along the plane of least resistance; however, other information can be gleaned from wet-fracturing (**Figure 8**). The fissures swell upon soaking and become more evident following fracture in whole grain cross sections of both CM101 (**Figure 8a**) and M202 (**Figure 8b**). Soaking CM101 grain increased spaces between starch granules and made central cavities more readily discernible (**Figure 8c**). Spaces occurred between individual starch granules in soaked, milled M202 grains. Because the fracture plane also went through starch granules in the soaked M202 grains (**Figure 8d**,**f**), it was evident that no central cavities occurred within the starch granules. Protein bodies were readily identified in soaked CM101 (**Figure 8e**).

To understand the behavior of isolated starch during gelatinization, milled grains were cooked and removed from the water at intervals. The microstructure of CM101 milled grain changes rapidly during cooking. Large and small air pockets, caused by local expansion of steam, were formed in CM101 toward the periphery of the grain during the early stages of cooking (**Figure 9a**). Toward the center of the grain, air pockets were more definitive and uniform in size and the matrix was smooth, without structural details (**Figure 9b**). Specific staining and light microscopy showed that the matrix material, as expected, was composed mostly of starch (**Figure 9c**), with some protein (**Figure 9d**). Specific localization of cell wall material indicated that the cell walls were relatively intact (**Figure 9e**), despite the very disorganized appearance by SEM (**Figure 9f**). Even though CM101 rapidly transformed during cooking, there were areas in some kernels in which starch granules remained relatively intact even after 20 min of cooking (**Figure 9g**),

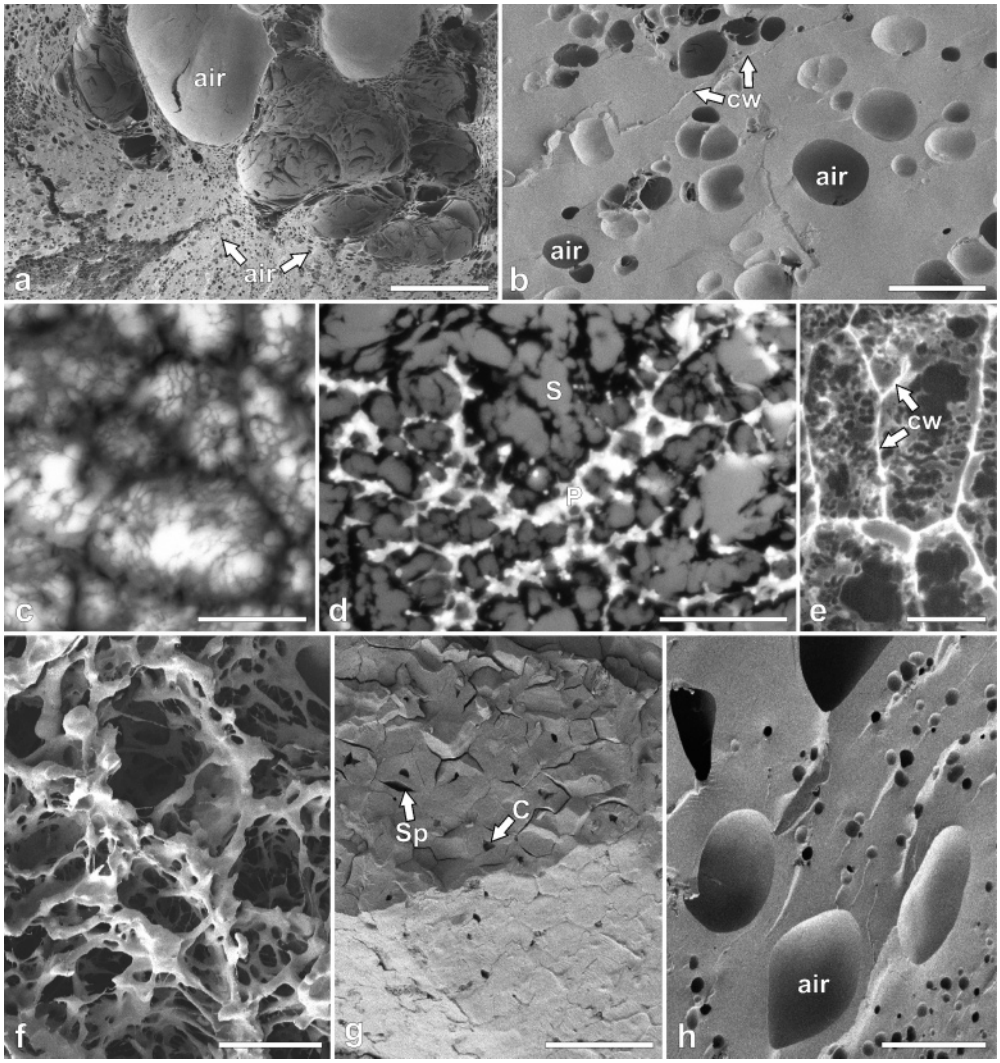

Figure 9. Micrographs of CM101 milled rice cooked for various times: 10 min (**a**–**d**), 15 min (**e**), 20 min (**f**–**h**). Large steam or air pockets and fine structure with small air pockets are evident toward the outside of the grain (**a**). A scanning electron micrograph (**b**) shows the center of a cooked grain with a smooth matrix and more evenly sized and definitive large air pockets and edges of apposing cells (arrows). A light micrograph shows a section toward the exterior of a grain that had been cooked for 10 min (**c**). The section stained reddish purple (light and dark gray) with I_2KI is a completely cooked area; white areas are unstained and indicate air (steam) pockets. (**d**) Section of milled rice cooked for 10 min and stained with Acid Fuchsin for protein and viewed under fluorescence illumination at 450–490 nm excitation (exciter filter, 450–490; beam splitter, FT 510; barrier filter, LP 520) shows protein distribution (brightest areas). The section was taken approximately midway between the outer and center portions of the grain. (**e**) A light micrograph shows a section toward the exterior of a rice grain that had been cooked 15 min. The section was stained with Congo Red and viewed using fluorescence microscopy (exciter filter, 390–420; beam splitter, FT 425; barrier filter, LP 450). Starch stains red (gray) and cell walls stain blue (white, denoted by arrows) due to autofluorescence. Unstained (black) areas are air pockets. (**f**) Areas comparable to panels **c** and **e** viewed by scanning electron microscopy show a stretchy, open structure suggesting a gummy, soft texture. (**g**) Scanning electron micrograph shows a milled grain cooked for 20 min. The area is virtually uncooked; starch granules with cavities are evident. (**h**) Scanning electron micrograph shows a grain cooked for 20 min; the area is completely cooked and shows a smooth matrix with large and small air pockets. C, cavity; cw, cell wall; P, protein; S, starch; Sp, space. Magnification markers: **a**, 100 μm; **b**–**d**, 10 μm; **e**, **f**, 25 μm; **g**, 10 μm; **h**, 5 μm.

whereas other areas were completely gelatinized into a smooth matrix in which large and small air pockets were embedded (**Figure 9h**). The scanning electron micrographs hint that CM101 has a soft, gummy texture. Similar microscopic observations were made by Sandhya Rani and Bhattacharya (*13*), who found that CM101 or low-amylose cooked rice with widespread granule disintegration was soft and sticky, whereas high-amylose cooked rice with less granule disintegration was hard and less sticky.

M202 maintained its integrity during cooking and did not form large air pockets. Toward the periphery, M202 grains exhibited a compact and dense structure after 10 min of cooking (**Figure 10a**). In the interior, there were unevenly cooked "raw" areas (**Figure 10b**,**c**), as in CM101. During cooking, amylose is leached from starch granules into the surrounding matrix and collects into pockets, as shown by I_2KI staining (**Figure 10d**). Areas of high amylose are darkly stained (*32*). A comparable area of high amylose accumulation is shown under SEM (**Figure 10e**). The air pockets were quite small and uniform in cooked M202 grains (**Figure 10e**). Protein was distributed in a linear fashion, and starch was mostly unstained by Acid Fuchsin (**Figure 10f**), unlike in CM101. In the center of the grain, air pockets were very small and also occurred linearly (**Figure 10g**). At the periphery of the grain, larger, less definitive, perhaps

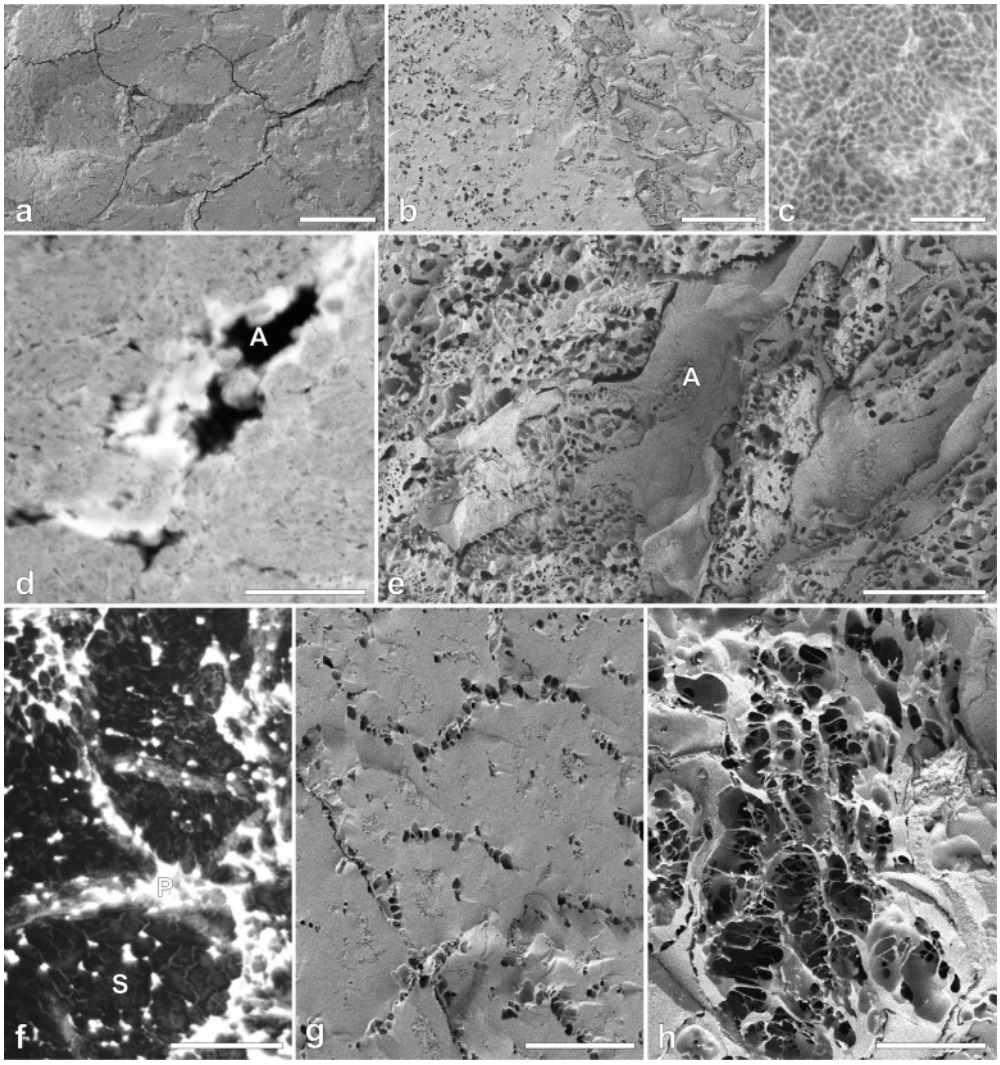

Figure 10. Cooked milled rice M202: **a**–**f**, cooked for 10 min; **g**, **h**, cooked for 20 min. (**a**) Scanning electron micrograph shows dense structure following cooking for 10 min. (**b**) Scanning electron micrograph shows a smooth region with small air pockets and the interface between two types of structures; one shows more "melting" (left) than the other. (**c**) Light micrograph section stained for starch with I_2KI shows incompletely cooked areas. (**d**) Light micrograph section stained with I_2KI shows light blue (gray) matrix and "pools" of dark blue (black) amylose. (**e**) Scanning electron micrograph of areas comparable to panel **d** shows that the "pool" of amylose has a dense structure. (**f**) Section stained with acid fushsin for protein shows the abundance of protein (white areas) and unstained starch structure. (**g**) Scanning electron micrograph near the center of a milled rice kernel cooked for 20 min shows a dense, smooth structure containing small air pockets that appear to be uniformly distributed. A, amylose "pool"; P, protein; S, starch; C, cavity; P, protein; S, starch; Sp, space. Scale bars: **a**, 50 μm; **b**, 10 μm; **c**, **d**, 50 μm; **e**–**g**, 5 μm; **h**, 10 μm. M202, note the lack of "melting" starch granules.

open-celled air pockets formed in the completely cooked grain (**Figure 10h**). The smaller air pockets had prickly looking fibrillar connections within the air pockets (**Figure 3b**).

Conclusions. Differences observed during SEM of raw and soaked milled grains suggest that the starch matrix of CM101 had a soft, open texture, whereas M202 rice was denser and firmer. Microscopy of cooked grains indicates that M202 has a firm texture and dense interior with small pockets uniformly spread throughout the matrix, indicating firm texture. Large, rounded air pockets, a tendency for starch granules to melt together, and a more open structure indicate that CM101 has a smooth, sticky, or gummy texture.

Both CM101 and M202 starches isolated with NaOH showed lower initial gelatinization temperatures and higher overall viscosities compared to their respective flours. Three methods of starch isolation were compared using M202 rice flour. Alkaline, detergent, and enzymatic treatments all effectively removed protein, but had variable effects on starch pasting properties. The rheological changes may be attributed to lipid removal by alkaline and detergent treatments. Lipid removal had a dramatic effect on pasting properties of isolated starches, decreasing initial gelatinization temperature and increasing overall viscosity. M202 starch obtained using Pronase, which did not reduce or disrupt lipids as much, showed smaller changes in initial gelatinization properties compared to M202 flour. These findings indicate that fats play a critical role in the pasting properties of rice flours and their respective starches.

LITERATURE CITED

(1) Biliaderis, C. G.; Juliano, B. O. Thermal and mechanical properties of concentrated rice starch gels of varying composition. *Food Chem.* **1993**, *48*, 243−250.

(2) Juliano, B. O. *Rice: Chemistry and Technology*; Juliano, B. O., Ed.; American Association of Cereal Chemists: St. Paul, MN, 1985.

(3) Champagne, E. T.; Bett, K. L., Vinyard, B. T.; McClung, A. M.; Barton, F. E., II; Moldenhauer, K.; Linscombe, S.; McKenzie, K. Correlation between cooked rice texture and Rapid Visco Analyser measurements. *Cereal Chem.* **1999**, *76*, 764−771.
(4) Tan, Y.; Corke, H. Factor analysis of physicochemical properties of 63 rice varieties. *J. Sci. Food Agric.* **2002**, *82*, 745−752.
(5) Martin, M.; Fitzgerald, M. A. Proteins in rice grains influence cooking properties! *J. Cereal Sci.* **2002**, *36*, 285−294.
(6) Lii, C.-Y.; Shao, Y.-Y.; Tseng, K.-H. Gelation mechanism and rheological properties of rice starch. *Cereal Chem.* **1995**, *72*, 393−400.
(7) Whistler, R. L.; BeMiller, J. N. Starch. In *Carbohydrate Chemistry for Food Scientists*; Eagan Press, American Association of Cereal Chemists: St. Paul, MN, 1997; pp 117−135.
(8) Perez, C. M.; Villareal, C. P.; Juliano, B. O.; Biliaderis, C. G. Amylopectin staling of cooked non-waxy milled rices and starch gels. *Cereal Chem.* **1993**, *70*, 567−571.
(9) Singh, V.; Okadame, H.; Toyoshima, H.; Isobe, S.; Ohtsubo, K. Thermal and physicochemical properties of rice grain, flour and starch. *J. Agric. Food Chem.* **2000**, *48*, 2639−2647.
(10) Maniñgat, C. C.; Juliano, B. O. Starch lipids and their effect on rice starch properties. *Starch* **1980**, *32*, 76−82.
(11) Lim, S.-T.; Tee, J.-H.; Shin, D.-H.; Lim, H. Comparison of protein extraction solutions for rice starch isolation and effects of residual protein content on starch pasting properties. *Starch* **1999**, *51*, 120−125.
(12) Sandhya Rani, M. R.; Bhattacharya, K. R. Rheology of rice-flour pastes: Relationship of paste breakdown to rice quality, and a simplified Brabender viscograph test. *J. Texture Stud.* **1995**, *26*, 587−598.
(13) Sandhya Rani, M. R.; Bhattacharya, K. R. Microscopy of rice starch granules during cooking. *Starch* **1995**, *47*, 334−337.
(14) Takeda, Y.; Maruta, N.; Hizukuri, S.; Juliano, B. O. Structures of indica rice starches (IR48 and IR64) having intermediate affinities for iodine. *Carbohydr. Res.* **1989**, *187*, 287−294.
(15) Maniñgat, C. C.; Juliano, B. O. Properties of lintnerized starch granules from rices differing in amylose content and gelatinization temperature. *Starch* **1979**, *31*, 5−10.
(16) American Association of Cereal Chemists. *Approved Methods of the AACC*, 10th ed.; AACC: St. Paul, MN, 2000; method 46-30.
(17) Gibson, T. S.; Solah, V. A.; McCleary, B. V. A procedure to measure amylose in cereal starches and flours with concanavalin A. *J. Cereal Sci.* **1997**, *25*, 111−119.
(18) Malvern Instruments Ltd. *MasterSizer Instruction Manual*, IM100, Issue 3; Malvern Instruments: Malvern, U.K., 1990.
(19) Yokoyama, W.; Renner-Nantz, J. J.; Shoemaker, C. F. Starch molecular mass and size exclusion chromatography in DMSO-LiBr coupled with multiple angle laser light scattering. *Cereal Chem.* **1998**, *75*, 530−535.
(20) Berry, G. C. Thermodynamic and conformational properties of polystyrene. I. Light-scattering studies on dilute solutions of linear polystyrenes. *J. Chem. Phys.* **1966**, *44*, 4550−4564.
(21) Fulcher, R. G.; Wong, S. I. Inside cereals—a fluorescence microchemical view. In *Cereals for Food and Beverages: Recent Progress in Cereal Chemistry and Technology*; Inglett, G. E., Munck, L., Eds.; Academic Press: New York, 1980; pp 1−26.
(22) Clark, G. I_2KI. In *Staining Procedures*, 4tn ed.; Williams and Wilkins: Baltimore, MD, 1981; pp 362−363.
(23) Revilla, N. A.; Tolivia, D.; Tarrage, J. F. A new and permanent staining method for starch granules using fluorescence microscopy. *Stain Technol.* **1986**, *61*, 151−154.
(24) Humphreys, W. J.; Spurlock, B. O.; Johnson, J. Critical-point drying of ethanol-infiltrated, biological specimens for scanning electron microscopy. *Scanning Electron Microsc.* **1974**, *1974*, 105−110.
(25) USDA. Nutrient Database for Standard Reference, release 13, 1999.
(26) Bean, M. M.; Esser, C. A.; Nishita, K. D. Some physicochemical and food application characteristics of California waxy rice varieties. *Cereal Chem.* **1984**, *61*, 475−480.
(27) Park, I.; Ibanez A. M.; Shoemaker, C. F. Rice starch molecular size and its relationship with amylose content. *Starch* **2007**, *59*, 69−77.
(28) Ogawa, Y.; Glenn, G. M.; Orts, W. J.; Wood, D. F. Histological structures of cooked rice grain. *J. Agric. Food Chem.* **2003**, *51*, 7019−7023.
(29) Lisle, A. J.; Martin, M.; Fitzgerald, M. A. Chalky and translucent rice grains differ in starch composition and strucutre and cooking properties. *Cereal Chem.* **2000**, *77*, 627−632.
(30) Huber, K. C.; BeMiller, J. N. Visualization of channels and cavities of corn and sorghum starch granules. *Cereal Chem.* **1997**, *74*, 537−541.
(31) Jane, J.-L.; Chen, Y. Y.; Lee, L. F.; McPherson, K. S.; Wong, M.; Radosavljevic, M.; Kasemsuwan, T. Effect of amylopectin branch chain length and amylose content on the gelatinization and pasting properties. *Cereal Chem.* **1999**, *76*, 629−637.
(32) Wood, D. F.; Yu, P. C.; Ibanez-Carranza, A. M.; Shoemaker, C. F. Microstructural changes in rice during cooking. In *30th Annual UJNR Symposium Proceedings*, Oct 14−20, 2001, Tsukuba, Japan, 2001; pp 278−283.

Received for review February 12, 2007. Revised manuscript received May 11, 2007. Accepted June 1, 2007.

JF070416X